International Journal of Pharmaceutics 421 (2011) 24–33

Contents lists available at SciVerse ScienceDirect

International Journal of Pharmaceutics

journal homepage: www.elsevier.com/locate/ijpharm

Multi-equilibrium system based on sertraline and β-cyclodextrin supramolecular complex in aqueous solution

Joel J. Passos[a], Frederico B. De Sousa[a], Ivana S. Lula[a], Elison A. Barreto[b], Juliana Fedoce Lopes[b], Wagner B. De Almeida[b], Rubén D. Sinisterra[a,*]

[a] Laboratório de Encapsulamento Molecular e Biomateriais (LEMB) – Departamento de Química, Instituto de Ciências Exatas, Universidade Federal de Minas Gerais (UFMG), Belo Horizonte 31270-901, MG, Brazil

[b] Laboratório de Computacional e Modelagem Molecular (LQC-MM) – Departamento de Química, Instituto de Ciências Exatas, Universidade Federal de Minas Gerais (UFMG), Belo Horizonte 31270-901, MG, Brazil

ARTICLE INFO

Article history:
Received 12 May 2011
Received in revised form 26 July 2011
Accepted 14 September 2011
Available online 22 September 2011

Keywords:
Sertraline
β-Cyclodextrin
Inclusion compound
Theoretical calculations
Physical–chemical parameters
Multi-equilibrium

ABSTRACT

Sertraline (SRT) is a widely used antidepressant whose poor solubility in water limits its oral applicability. Thus, the aim of this work was the evaluation of a multi-equilibrium system based on β-cyclodextrin (βCD) and SRT. The inclusion compounds (ICs) were investigated by infrared spectroscopy, isothermal titration calorimetry (ITC) and ^{1}H and 2D ROESY nuclear magnetic resonance experiments. SRT solubility was predicted *in vitro* in water and biomimetic fluids. The SRT in presence of βCD at 1:1 and 1:2 molar ratios was more soluble than free SRT in all biomimetics media investigated. The FTIR-HATR showed that βCD νC–O–C stretching band was reduced in presence of SRT, suggesting the interactions between them. Additionally, titration process and Job's plot provided information on the ICs stoichiometry and evidenced the multi-equilibrium coexistence in aqueous solution. According to the ITC, SRT:βCD interaction process was spontaneous and exothermic with a high affinity binding constant ($K = 14{,}726\ M^{-1}$). Additionally, the stoichiometry coefficient (*n*) was 1.63, which was comparable to that found by FITR-HATR. The ^{1}H and 2D ROESY verified multiple SRT sites included into the host cavity. Theoretical calculations depicted the relative energy of different proposed ICs structures, in which the 1:2 IC was the most stable.

1. Introduction

Sertraline hydrochloride (SRT), Fig. 1a, is a selective serotonin reuptake inhibitor used for treatment of several disorders such as depression, obsessive–compulsive, social phobia, panic, anxiety and eating issues. SRT is also the second most potent serotonin reuptake inhibitor and one of the top ten pharmaceutical products sold worldwide (Nouws et al., 2005). It is known that SRT presents drawbacks, namely slow oral absorption, lower oral bioavailability due to its low solubility (3.8 mg mL^{-1}) (Johnson et al., 1996). Solubility is a fundamental parameter in screening for drug absorption effective in the clinical response for almost all drugs given orally. Oral activity is obtained by dissolution of the drug and its bioavailability depends on the drug behavior in the gastrointestinal tract (Hörter and Dressman, 2001). Studies have shown that more than 40% of drugs failures are due to poor bioavailability, which is a consequence of either low solubility or permeability or even both (Panchagnula and Thomas, 2000).

Based on the biopharmaceutical drug classification, SRT belongs to Class II, i.e. low solubility and high permeability (Sutton et al., 2006). To circumvent these drawbacks and to increase drug aqueous solubility, cyclodextrins (CDs) have been used as an efficacious strategy for several systems (Brewster and Loftsson, 2007; Davis and Brewster, 2004). Although CDs have been applied in different areas of science as biomaterials and drug delivery systems (Davis and Brewster, 2004; De Sousa et al., 2010b; Harada et al., 2011), the pharmaceutical interest in these molecules have arisen based on their ability to modify chemical, physical and biological properties of the guest molecules through inclusion compound (IC) formation (De Sousa et al., 2010a; Marques et al., 2011; Uekama et al., 1998). Additionally, CDs are able to improve solubility, stability and consequently the bioavailability of the guest drug inserted into their cavities (Loftsson and Duchene, 2007).

CDs molecules are composed mainly of 6, 7 or 8 glucopyranose linked by α-(1,4) glucosidic units, named α-, β-, γ-cyclodextrin, respectively. CDs have a torus shape, Fig. 1b, providing a hydrophobic cavity, while the hydroxyl groups located outside present a hydrophilic character to this part of the molecule (Szejtli, 1998). This feature allows CDs to form ICs, trapping a variety of guest molecules into their cavity (Szejtli, 1998; Uekama et al., 1998). It has been reported in the literature the coexistence of multiple inclusion

* Corresponding author. Tel.: +55 31 3409 5778; fax: +55 31 3409 5700.
E-mail address: sinisterra@ufmg.br (R.D. Sinisterra).

0378-5173/$ – see front matter © 2011 Elsevier B.V. All rights reserved.
doi:10.1016/j.ijpharm.2011.09.026

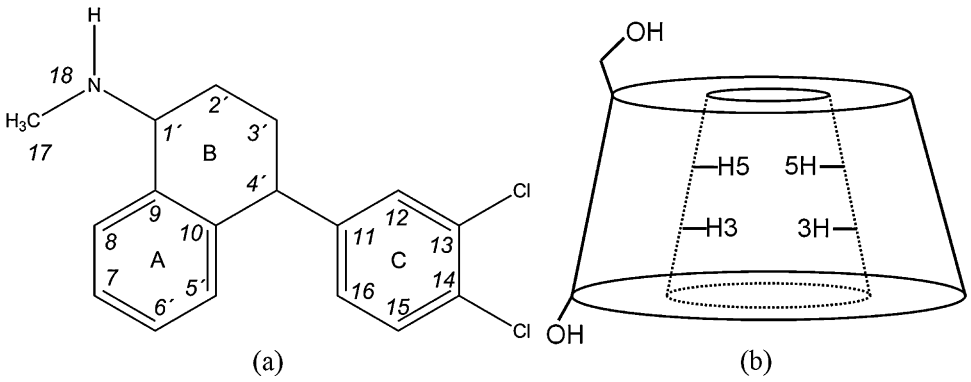

Fig. 1. (a) Sertraline molecular structure and (b) βCD schematic structure.

modes of the guest molecules into the CD cavity in aqueous solution (De Sousa et al., 2008b; Messner et al., 2010). In this sense, a careful physical–chemical characterization concerning the supramolecular complex stoichiometry, binding sites and three-dimensional arrangement can provide highly important information, helping to choose the best drug:CD ratio, which might lead to a better drug activity.

Herein, we report the ICs characterization formed between SRT with βCD at 1:1 and 1:2 molar ratios prepared by freeze-drying (FD) method in order to improve the guest molecule solubility in aqueous medium. The supramolecular system ratio was chosen based on the SRT possible binding sites with the βCD molecule. To study the changes in the SRT solubility after its interactions with βCD, equilibrium solubility experiments were carried out. SRT:βCD was investigated using different physical–chemical approaches in aqueous solution to get insights about the supramolecular complex arrangement, stoichiometry and binding constant.

2. Materials and methods

2.1. Materials

Sertraline hydrochloride monohydrated was kindly given by Medley Pharmaceutical CO. S/A. β-cyclodextrin (βCD) was acquired from CERESTAR, USA.

2.2. Preparation of SRT:βCD inclusion compound by freeze drying (FD)

The ICs were prepared mixing SRT and βCD aqueous solutions at 1:1 or 1:2 molar ratios. The SRT was added into the βCD aqueous solution and the final solution was kept under stirring for 4 h at room temperature. Then, the ICs solutions were frozen in liquid nitrogen and freeze-dried in a Thermo Electron Co. Equipment, Savant ModulyD. In order to verify the influence of the preparation process on the SRT solubility, free SRT aqueous solution was submitted to FD process.

2.3. Equilibrium solubility (shake-flask method)

Equilibrium solubility study of free SRT and ICs was carried out at 37 °C in the following dissolution media: water, simulated gastric fluid (SGF) and simulated intestinal fluid (SIF). The SGF medium is HCl/KCl (0.05 mol L^{-1}) acid buffer solution at pH 2.0, while SIF is a phosphate buffer solution (0.05 mol L^{-1}) at pH 7.5 and both media were prepared in absence of enzyme. Excess of SRT or ICs were added into Eppendorf® tubes with 1.5 mL of dissolution medium. These aqueous suspensions were shaken at 60 rpm at 37 °C for 48 h until solid/liquid equilibrium had been achieved (Baka et al., 2008). The suspension was centrifuged at 12,000 rpm and filtered with a 0.22 μm Millipore® membrane filters. SRT concentration in the filtrate was determined at λ 274 nm using an UV–vis HP 8453 spectrophotometer using quartz cuvette with 1.0 cm optical path. These UV–vis method used to quantify the SRT was linear in the range of 0.08–0.40 mg mL^{-1}, in accordance with the calibration curves (see figures in Supplementary Data 1), with linear fitting values "*r*" higher than 0.99. The limit of detection (LOD) was determined by spectrometric analysis at λ 274 nm of 10 blank samples measurements, which was spiked with low concentration of SRT (0.010 mg mL^{-1}). LOD values were 0.0006, 0.0010 and 0.0009 mg mL^{-1} for water, KCl/HCl and PBS, respectively. Limit of quantification (LOQ) were 0.0019, 0.0033 and 0.0030 mg mL^{-1} in water, KCl/HCl and PBS. The experiments were carried out for free SRT and SRT submitted to the FD process (SRTFD), as well as to the SRT:βCD ICs obtained by this method at 1:1 and 1:2 molar ratios. These experiments were carried out in triplicate.

2.4. FTIR-HATR measurements

FTIR-HATR spectra of the βCD, SRT and titration of βCD in SRT in aqueous solution were obtained using a Perkin Elmer spectrophotometer model, Spectrum GX equipped with reflection accessory in a ZnSe crystal. All spectra were recorded between 4000 and 400 cm^{-1} with 4 cm^{-1} and 32 scans per measurement. After data acquisition, all spectra were subtracted from MilliQ® water spectrum to reduce the water bands stretching influences. The ICs stoichiometry was predicted by titration and continuous variation method (Job's plot). In both methods, the stoichiometry was estimated using the βCD νC–O–C stretching band at 1031 cm^{-1} in presence and absence of SRT (De Sousa et al., 2008c).

In the titration process, βCD aqueous solution at 12.0 mmol L^{-1} was titrated with SRT aqueous solution at 5.0 mmol L^{-1} and the final concentration of both molecules varied from 1.1 to 6.0 mmol L^{-1} and 4.5 to 2.5 mmol L^{-1}, respectively. The difference of βCD νC–O–C stretching at 1031 cm^{-1} ($\Delta\nu$C–O–C) in the presence and absence of SRT were plotted *versus* molar ratio ([βCD]/[SRT]).

In addition, the stoichiometry was investigated by Job's plot. This method involves the mixture of equimolar aqueous solutions keeping total molar concentration constant, however, the molar fractions ([βCD]/[βCD]+[SRT]) varied from 0 to 1.0. According to the continuous variation method, the maximum value observed in the Job's plot ($\Delta\nu$C–O–C against [βCD]/[βCD]+[SRT]) represents the most favorable IC stoichiometry in solution (de Araujo et al., 2007). Therefore, βCD aqueous solution at 10.0 mmol L^{-1} was mixed with different volumes of SRT solution aqueous at 10.0 mmol L^{-1}, in which molar fraction varied from 0.1 to 0.9. The experiments were carried out at room temperature in triplicate.

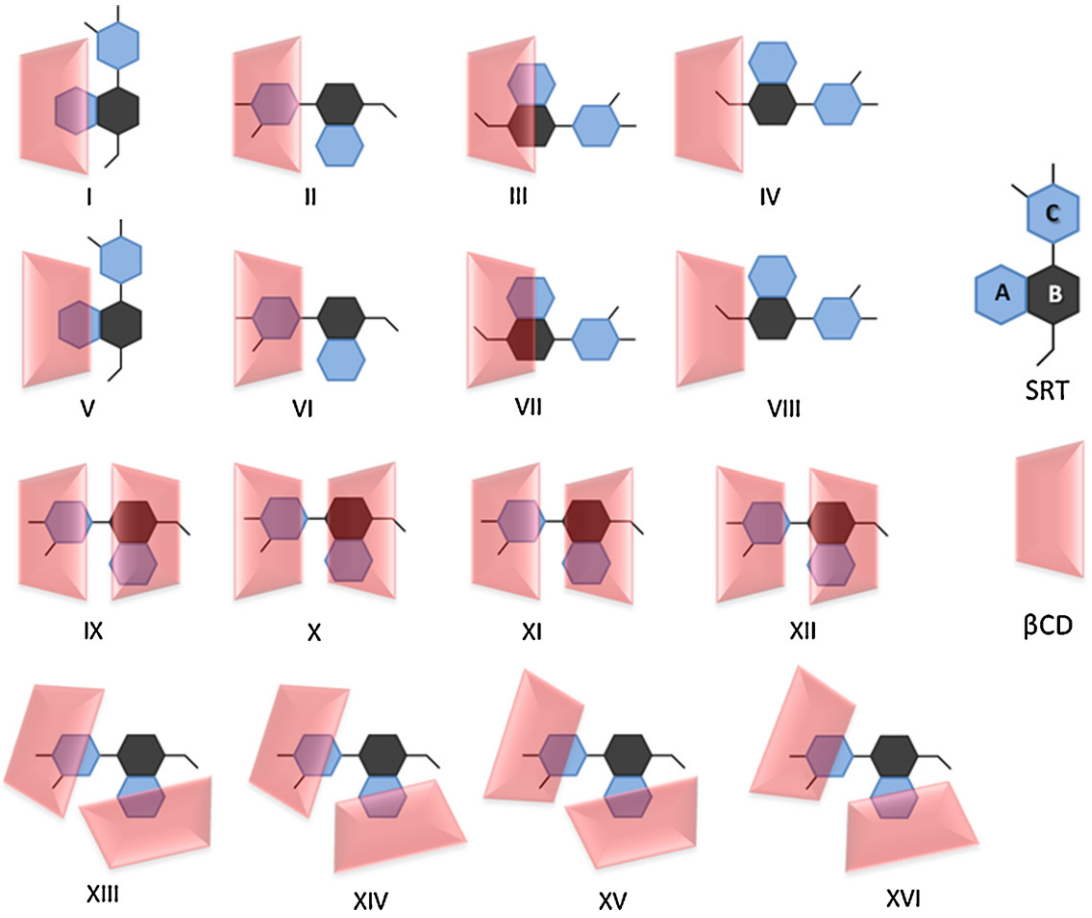

Fig. 2. SRT/βCD inclusion modes evaluated by theoretical calculations.

2.5. Isothermal titration calorimetry (ITC)

SRT:βCD thermodynamic parameters of interaction were identified using a NanoITC 2G TA Instruments at 25 °C by measuring the reaction heat flow released. Each titration was carried out as 50 successive injections of 5 μL of βCD aqueous solution at 14.0 mmol L^{-1} into the reaction calorimetric cell, which contained 1.2 mL of SRT aqueous solution at 1.0 mmol L^{-1}. The first injection of 1 μL was discarded to eliminate diffusion effects of the syringe material into the calorimetric cell. The interval of 600 s was used, which was sufficient to achieve equilibrium and signal return to baseline and stirring in the calorimetric cell was kept constant 250 rpm. The reference calorimeter cell was loaded with 1.2 mL of MilliQ® water and kept closed during the experiments. SRT and βCD concentration into the calorimetric cell varied from 1.0 to 0.79 mmol L^{-1} and 0.0 to 2.9 mmol L^{-1}, respectively. The dilution processes were carried out of βCD aqueous solution into pure water and pure water into the SRT aqueous solution, which were used to subtracted from the SRT:βCD titration curve. The calorimetric data were assay by NanoAnalyze software supplied with equipment and the standard enthalpic variation (ΔH^o), stoichiometry (n) and binding constant (K) obtained using the *independent model* from software. The standard Gibbs free energy (ΔG^o) and standard entropy variation ($T\Delta S^o$) were calculated from titration data.

2.6. Nuclear magnetic resonance (NMR)

NMR is powerful tool to study drug:CD interactions, allowing to define the sites of interaction between host and guest molecules. NMR spectra were obtained in a Bruker DPX-400 AVANCE operating at 400 MHz, using D_2O (Cambridge isotopic 99.9%) as solvent at 27 °C. One-dimensional ^1H NMR experiment was performed with 5 mm dual probe using direct detection with z-gradient coil and WATERGATE technique for suppression of the residual water signal. The 2D ROESY experiment was recorder using the inversion-recovery sequence (90-t-180). The standard experimental parameters of the spectrometer library was applied with mixing time of 600 ms. The concentration of free SRT solution was 2.0 mg mL^{-1}, due to low solubility. All ICs solutions were taken in the match concentration of free SRT solution. The water signal was used to reference (Gottlieb et al., 1997).

2.7. Theoretical calculations

Starting structure for the βCD was obtained by the X-ray structure deposited as code BCDEXD10 ((CSD):http://www.ccdc.cam.ac.uk/) at the Cambridge Structural Database available for βCD hydrated (Lindner and Saenger, 1982). The water molecules present in this crystal structure were excluded for all calculations following the same procedure from our previous works (De Sousa et al., 2008a). SRT crystal structure was also used as the initial geometry (Caruso et al., 1999). The isolated molecules were fully optimized at DFT (Burke et al., 1988) level using the PBE1PBE (Perdew et al., 1996, 1997) functional with the Pople's standard split valence 6-31G(d,p) basis set (Hehre et al., 1972). Vibrational analysis was also performed for the characterization of the optimized structures as true minima on the potential energy surface (PES).

SRT structure has two planar phenyl rings (A and B) in its molecular structure that are closely orthogonal to each other and connected by an unsaturated ring (C). This ring is in a chair

conformation and it is also bonded to the methyl ammonium chloride structure as showed in Fig. 1a. The SRT chemical arrangement with the narrower and wider rims of βCD, and also the two different stoichiometries investigated provide 16 possible geometrically distinct ICs as can be seen in Fig. 2. For the designed supramolecular ICs, the geometry optimizations were first carried out at the PM3 (Stewart, 1989) level semiempirical level. For the PM3 most stable ICs geometry optimizations were carried out at the DFT level with the PBE1PBE (Perdew et al., 1996, 1997) functional using the 6-31G(d,p) (Ditchfield et al., 1971) basis set followed by harmonic frequency calculations, which has a high computational cost, specially for the 1:2 IC stoichiometry. The solvent effect was taken into account following the integral equation formalism polarized continuum model (IEFPCM) (Cances et al., 1997). This method describes the condensed phase as a classical electronic medium represented by the solvent dielectric constant (for water $\varepsilon = 78.39$). The solute molecule is placed in a suitable cavity to enclose the entire molecule. The solute cavities for all structures were described by the Universal Force Field (UFF) atomic radii. All theoretical calculations were carried out using Gaussian 2003 (Frisch et al., 2004) suite of computational chemistry programs.

3. Results and discussion

3.1. Equilibrium solubility shake flask method

In a broad sense, solubility may be defined as the amount of substance that dissolves in a given volume of solvent at a specified temperature. The SRT molecule is poorly soluble in water, and according to literature, its solubility depends on pH of the medium (Johnson et al., 1996). In order to quantify the SRT solubility after its interaction with βCD, equilibrium solubility of ICs were measured in gastrointestinal biomimic fluids and water. Thus, to determine the equilibrium solubility of free SRT, SRTFD and SRT in the ICs at 1:1 and 1:2 molar ratios were carried out.

Free SRT solubility in water is 4.0 ± 0.23 mg mL^{-1} in accordance to reported in the literature, which is 3.80 mg mL^{-1} (Johnson et al., 1996). SRT solubility in the ICs at 1:1 and 1:2 molar ratios using water as solvent were 25.60 ± 0.75 and 32.0 ± 0.60 mg mL^{-1}, which represents a solubility increases of six and eight times higher than SRT, respectively. These SRT increased solubility in presence of βCD is an evidence of the interaction between both molecules in aqueous solution. However, water solubility does not represent the gastrointestinal tract conditions, mainly pH medium. Thus, to simulate these conditions, SRT solubility was measured in SGF and SIF biomimetic fluids, which is given at specific buffered pH (Hörter and Dressman, 2001). It is clear that the SRT, in presence of βCD, was more soluble than free SRT under those tested conditions. SRT solubility of at 1:1 and 1:2 molar ratios in SGF medium are 5.0 ± 0.93 and 12.80 ± 0.65 mg mL^{-1}, respectively, which were higher than free SRT in the same solvent (1.5 ± 0.05 mg mL^{-1}). These results showed that SRT solubility enhanced after βCD interaction using biomimetic gastric fluid.

Although free SRT and SRT in presence of βCD present lower solubility in SIF medium compared to water and SGF media, SRT solubility values at 1:1 and 1:2 molar ratios in SIF medium are 0.80 ± 0.10 and 1.0 ± 0.37 mg mL^{-1}, while the free SRT solubility is 0.3 ± 0.03 mg mL^{-1}. The low solubility of SRT in SIF medium may be due to the increase of the pH, where the predominant species in solution is the SRT non ionized form. The SRT is weak acid (pK_a 9.16) and is soluble in low pH solutions due to the protonated secondary amino group, on the other hand, increasing the pH medium favors the SRT non protonated form, which is less soluble (Takács-Novák et al., 2006). However, comparing the SRT solubility of free molecule and its ICs at 1:1 and 1:2 molar ratios it was observed enhancement of 166 and 233%in SIF medium, respectively.

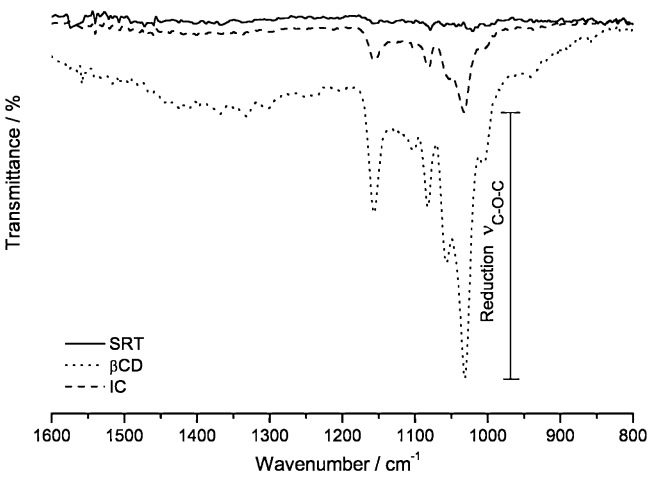

Fig. 3. FTIR-HATR of spectra of free SRT (3.3 mmol L^{-1}), βCD (3.3 mmol L^{-1}) and SRT:βCD IC at 1:1 molar ratio in the region of 1600–800 cm^{-1}.

In order to study the influence of the FD process in drug solubility, SRT solubility was also investigated in the absence of βCD after this process, SRTFD. SRTFD solubility values in water, SGF and SIF dissolution media are 5.6 ± 0.21, 1.8 ± 0.16 and 0.6 ± 0.03 mg mL^{-1}, respectively. It is clear that the FD process increases the SRT solubility in range from 20, 25 and 100% in water, SGF and SIF medium, when compared to free SRT in the same media. This increase in the SRTFD solubility may be due to changes in molecular features of the sample, such as crystallinity, porosity and polymorphism (Baka et al., 2008). However, the increase in SRT solubility after interaction with βCD was more pronounced than observed after FD process, demonstrating the interaction between host and guest molecules.

According to solubility definitions and provisional biopharmaceutical classification reported in the literature, SRT is classified at slightly soluble compound, which range from 1 to 10 mg mL^{-1} (Sutton et al., 2006). SRT solubility at 1:1 molar ratio is 25.6 ± 0.76 mg mL^{-1}, which changes of the molecule solubility classification from slightly soluble to sparingly soluble (range from 10 to 33 mg mL^{-1}). Furthermore, the solubility of SRT at 1:2 molar ratio is 33.2 ± 0.60 mg mL^{-1}, which can be classified as soluble (range from 33 to 100 mg mL^{-1}), according the literature. Finally, analyzing these results, SRT:βCD system at 1:2 molar ratio has proved to have a higher solubility than 1:1 IC in all solvents evaluated, suggesting that increasing the βCD molar ratio can favor the SRT solubility.

3.2. FTIR-HATR measurements

FTIR-HATR has been applied to host-guest spectroscopy evaluation, allowing the characterization of system in solid state (Cannavà et al., 2008). However, spectroscopic technique has been recently used to demonstrate the host-guest interaction between drug:CD complex in aqueous solution. Additionally, stoichiometry of drug:CD complex in solution can be achieved using two methods: titration and continuous variation method (Job's Plot) (De Sousa et al., 2008b).

SRT and βCD FTIR-HATR spectra in aqueous solutions were monitored in the range of 1600–800 cm^{-1} to prevent the OH stretching bands interference. SRT spectrum at 3.3 mmol L^{-1} aqueous solution did not present any detectable bands around 1600–800 cm^{-1}, according to Fig. 3. The absence of SRT bands at this wavenumber may be due to the low SRT concentration in bulk solution. On the

contrary, free βCD aqueous solution at 3.3 mmol L^{-1} presents the characteristic νC–O–C stretching band at 1031 cm^{-1}, Fig. 3. When comparing the vibrational modes at 1031 cm^{-1} of the βCD in presence and absence of SRT in an equimolar ratio, it was observed a strong intensity reduction of the νC–O–C stretching, Fig. 3. This result can be attributed to the exchange of water molecules inside of βCD cavity for the guest molecule, which can restrict α-(1–4) νC–O–C vibrational freedom. This observation is in accordance with previous one observed by De Sousa and coworkers, which is an evidence of the interaction between drug and CD (De Sousa et al., 2008a).

FTIR-HATR spectrum of βCD during the titration process in water was monitored in a range of 1600–800 cm^{-1}. Dependence between νC–O–C stretching at 1031 cm^{-1} and the βCD concentration was observed (see figure in Supplementary Data 2). However, when βCD aqueous solution was titrated in SRT aqueous solution at 5.0 mmol L^{-1}, an intensity decrease of the νC–O–C stretching band was verified (see figure in Supplementary Data 3). These results can be better summarized in titration plot of βCD with SRT aqueous solution, which depicts the Δ νC–O–C stretching at 1031 cm^{-1} against molar ratio ([βCD]/[SRT]), Fig. 4a. This titration was adjusted to a nonlinear fitting. This nonlinear profile could be attributed to the host-guest weak interactions, observed in supramolecular systems, which are derived from the different interactions between host and guest molecules. Additionally, an inflection point around 1.56 is observed, suggesting that an equilibrium between different supramolecular systems can be observed in solution. In order to estimate the IC stoichiometry, the continuous variation method was carried out and the result is showed in Fig. 4b.

Fig. 4b presents a maximum molar fraction around 0.60 indicating that supramolecular species with molar ratio stoichiometry higher than 1:1 can be favored in solution among other supramolecular arrangements. However, coexistence of less favored stoichiometries should not be discarded, since titration method presents a factionary molar ratio. FTIR-HATR methods provided evidences about the SRT and βCD interactions, demonstrating the coexistence of different stoichiometries in solution. However, the FTIR-HATR technique is not the most precise tool to identify the supramolecular system stoichiometry based on weak intermolecular forces involving CDs. In order to evaluate the thermodynamic parameters of the SRT:βCD IC system, calorimetric measurements were carried out by ITC.

3.3. Isothermal titration calorimetry (ITC)

The interaction of host and guest molecules results in an enthalpy change, which can be detected by ITC. The interaction process can be exothermic or endothermic, according to the supramolecular system affinity (Sun et al., 2006a). The heat flow of βCD titration into the SRT solution is shown in Fig. 5a. The heat flow profile indicates that SRT:βCD interaction process is exothermic, since heat flow increases during the titration process. The heat output after each injection of βCD was determined by integrating each peak *versus* time, and plotting the data against the molar ratio. The heat flow of the βCD and SRT dilution process in water did not present enthalpy variation, Fig. 5b.

Based on these experiments, standard enthalpy change (ΔH^o), equilibrium constant (K_i) and stoichiometry coefficient (n) were obtained by NanoAnalyze® software, applying *independent model* fitting. The standard Gibbs free energy change (ΔG^o) and entropy effect ($T\Delta S^o$) was derived according to Eqs. (1) and (2), respectively.

$$\Delta G^o = -RT \ln K_i \quad (1)$$

$$\Delta G^o = \Delta H^o - T\Delta S^o \quad (2)$$

ITC stoichiometry coefficient value ($n = 1.62$) obtained by *independent model* fitting is close to the stoichiometry coefficient estimated using FTIR-HATR titration method ($n = 1.56$). This result obtained by ITC reinforces the FTIT-HATR capacity to identify the supramolecular system stoichiometry in solution. Moreover, ITC n value suggests that a higher supramolecular system than 1:1 molar ratio in solution must be consider as a stable IC.

The experimentally determined ΔH^o is −8.7 kJ mol^{-1} and represents the energy released during IC formation, Fig. 5c. The negative enthalpy value could be attributed to guest interaction with βCD through the weak supramolecular forces, such as van der Waals, hydrophobic interaction, hydrogen bond and electrostatic interactions (Sun et al., 2006b). These interactions were reported in other supramolecular host-guest systems and in general it is associated to the aromatic ring insertion into the βCD cavity (Bouchemal, 2008).

Furthermore, the IC formation could be aided to entropy contribution ($T\Delta S^o$). The entropy change during the IC formation was evaluated having a positive value, $-T\Delta S^o = -15.10$ kJ mol^{-1}, Fig. 5c. The positive entropy effect may be due to entropy compensation, which is a result of the negative contribution of host-guest interactions (conformational restriction) and the positive contribution of the water molecules release from the βCD cavity (Rekharsky and Inoue, 1998). Usually, hydrophobic interactions are governed by entropy, this occurs when enthalpy contributions is lower than entropy effect according to $|\Delta H^o| < |T\Delta S^o|$. On the other hand, van der Waals interactions forces is enthalpy driven and could be or not aided by entropy, $|\Delta H^o| > |T\Delta S^o|$ (Bouchemal, 2008). Thus, when compared to lower enthalpy variation ΔH^o |8.7 kJ mol^{-1}|and higher entropy contribution $T\Delta S^o$ |15.10 kJ mol^{-1}| can be concluded that SRT:βCD complexation was driven by entropy and aided by hydrophobic interactions, Fig. 5c. The positive entropy effect shows more greatly contributes to negative standard Gibbs free energy ΔG^o compared to the heat effect. The standard Gibbs free energy is negative $\Delta G^o = -23.80$ kJ mol^{-1} indicating that SRT:βCD interaction in aqueous solution is spontaneous, Fig. 5c.

Additionally, a high binding constant formation value was observed, $K_i = 14{,}726\ M^{-1}$, suggesting the large affinity between SRT and βCD. Thus, negative ΔG^o and high K_i value confirm that SRT:βCD interacts in aqueous solution. Despite the fact that the calorimetry experiments indicate the type of interactions in host-guest system, it is not possible through the thermodynamics parameters define the interaction binding sites of the supramolecular system, which can be determined through NMR experiments.

3.4. Nuclear magnetic resonance (NMR)

NMR spectroscopy has been used to establish inclusion geometry and ICs stoichiometry. Guest molecule included into the βCD cavity can change the dipolar moment of both molecules, leading to a hydrogen chemical shift. These results can be used as probe of host-guest interaction. Fig. 6 shows the ^{1}H NMR spectra of SRT dissolved in D_2O in absence and presence of βCD and Table 1 summarizes the chemical shifts values of the host and guest hydrogens. The δ_H values observed for free βCD are in agreement with those reported in the literature (Schneider et al., 1998). ^{1}H NMR spectrum of free SRT in D_2O, Fig. 6a, shows all SRT hydrogens: the aliphatic ones H1′, H2′, H3′, H4′ and H17 and those aromatic, which can be better depicted in Fig. 6b. Hydrogens H8, H15 and H6′, H7, H12 of the aromatic region are overlapped, however, it is important to emphasize that H5′and H16 are bonded in aromatic rings A and C, respectively.

Fig. 6c and d present the ^{1}H NMR spectra of the SRT:βCD IC at 1:1 molar ratio. It can be observed a chemical shift change ($\Delta\delta$) for all hydrogen in the IC spectrum compared to the free SRT spectrum. A higher variation in the NMR $\Delta\delta$ was observed for the SRT aromatic hydrogens in presence of βCD, Fig. 6d. The $\Delta\delta$ for host and guest

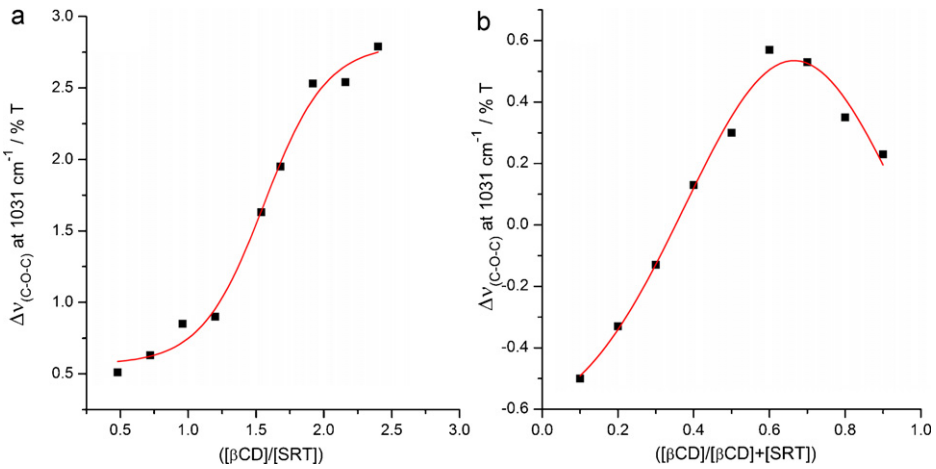

Fig. 4. FTIR-HATR experiments: (a) titration plot of βCD (12 mmol L^{-1}) with SRT (5.0 mmol L^{-1}) obtained using transmittance values at 1031 cm^{-1} and (b) continuous variation method (Job's plot).

molecules are presented in Table 1. SRT $\Delta\delta$ values of the H5′and H16 aromatic hydrogens are, respectively −0.114 and 0.094 ppm and this variation suggests that the SRT interaction with βCD can occur with two different guest molecule sites. Comparing H2′and H3′ $\Delta\delta$ values of IC and free SRT aliphatic hydrogens the $\Delta\delta$ was 0.137 and 0.156 ppm. These results suggest that aliphatic hydrogens were affected by changing the chemical environment around SRT molecule. On the other hand, aliphatic hydrogens H1′, H4′ and H17 were less affected than H2′and H3′ in presence of βCD. The aromatic hydrogen H8, H15, H6′, H7 and H12 were overlapped and the $\Delta\delta$ of chemical shift were not calculated.

One of the best probes to study drug:CD interactions is the $\Delta\delta$ of the H3 and H5 located inside the CD cavity, as depicted Fig. 1b (Fernandes et al., 2003). Chemical shift change in of the hydrogens H3 and H5 suggest the partial or entire insertion of drug in the βCD cavity (Schneider et al., 1998). IC $\Delta\delta$ in values of the H3 and H5

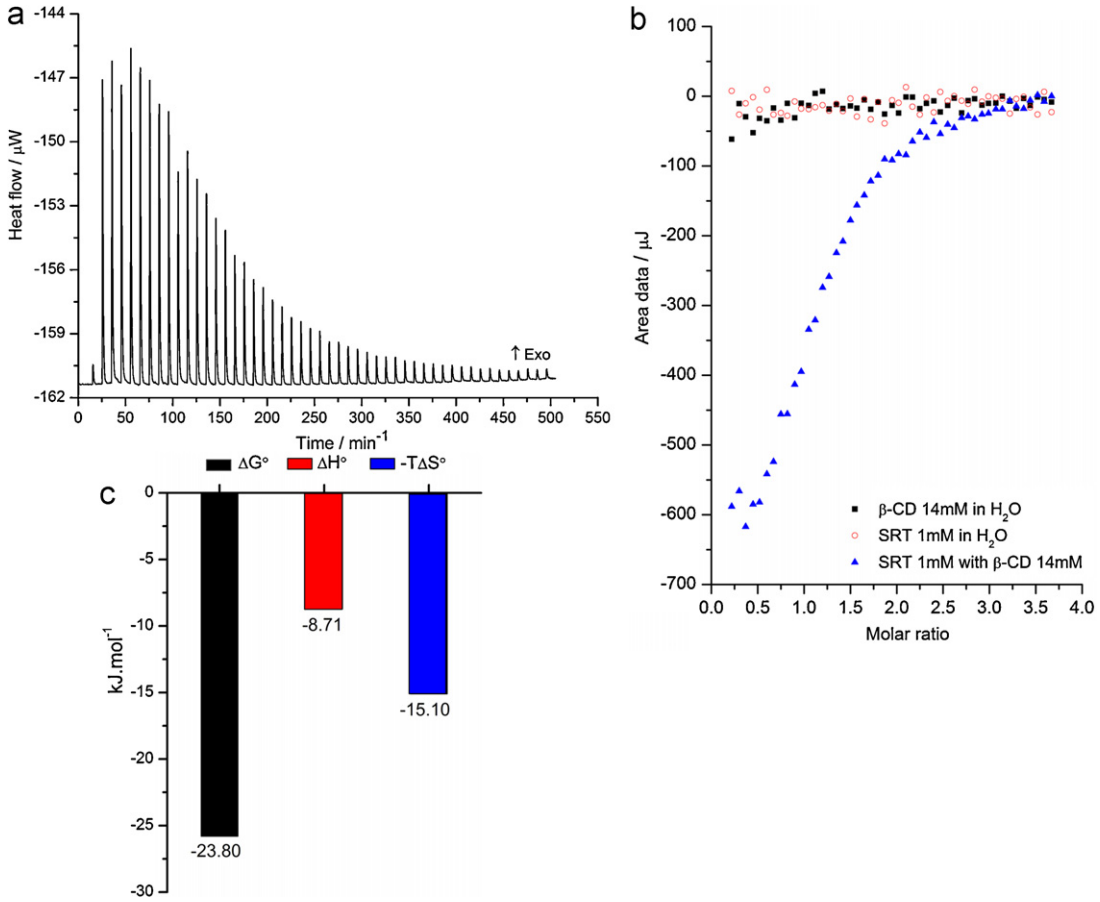

Fig. 5. ITC titration of SRT solution 1.0 mmol L^{-1} with βCD solution 14.0 mmol L^{-1} at 25 °C: (a) heat flow (μW) *versus* time, (b) titrations curves water in SRT aqueous solution (○), βCD aqueous solution in water (■) and SRT in βCD (▲) (subtracted from blank experiments), (c) standard Gibbs free energy, standard enthalpy change and standard entropic change values (in units of kJ mol^{-1}).

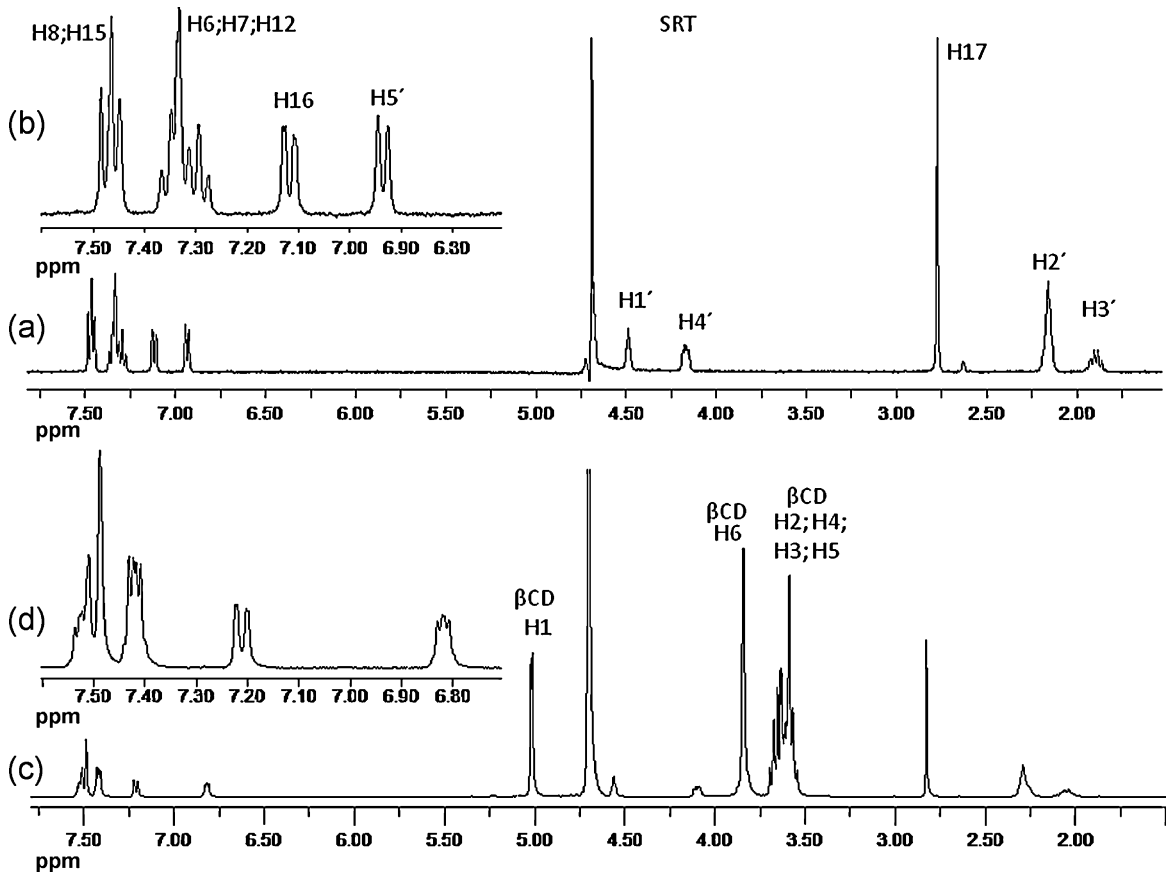

Fig. 6. ^{1}H NMR spectra in D_2O (400 MHz) of (a) free SRT, (b) expansion of free SRT from δ 6.70 to 7.60, (c) SRT:βCD IC at 1:1 molar ratio and (d) expansion of IC from δ 6.70 to 7.60.

Table 1
^{1}H NMR chemical shifts (ppm) of free SRT, βCD and SRT:βCD IC at 1:1 molar ratio at 27.0 °C (400 MHz, in D_2O).

^{1}H chemical shift δ/ppm			
	*δH	δH IC**	Δδ
SRT			
H1′	4.490	4.561	0.071
H2′	2.150	2.287	0.137
H3′	1.896	2.052	0.156
H4′	4.168	4.104	−0.064
H5′	6.934	6.820	−0.114
H8; H15	7.498–7.431	7.566–7.444	n.c.
H6;H7;H12	7.383–7.261	7.443–7.352	n.c.
H16	7.117	7.211	0.094
H17	2.774	2.828	0.054
β-CD			
H1	5.030	5.016	−0.014
H2	3.610	3.634	0.024
H3	3.930	3.660	−0.257
H4	3.550	3.566	0.016
H5	3.840	3.585	−0.255
H6	3.800	3.842	0.042

n.c., Δδ not calculated.
* Free SRT and β-CD hydrogens.
** IC-SRT:β-CD IC at 1:1molar ratio prepared by FD.

are, respectively −0.257 and −0.255 ppm, while H6 located at rim is less affected and presents the Δδ 0.042 ppm. The results obtained comparing the Δδ values indicated the interaction between both molecules in solution. The host–guest system formed to drug:CD are driven by weak intermolecular forces and Δδ of H3 and H5 could be explained by replacement of high energy water molecules inside the cavity by the guest molecule and the change in electronic density upon the inclusion process (Denadai et al., 2007; Sun et al., 2006a). However, ^{1}H NMR spectrum is not the best tool to study spatial interaction between the hydrogens in host–guest system.

In this sense, Nuclear Overhauser Effect (NOE) has been extensively used to study IC spatial correlations in short distance. The 2D rotating frame NOE (ROESY) is a powerful method to study spatial relationship in host–guest systems whose hydrogens are coupled in short distances, smaller than 5 Å (Jullian et al., 2008). ^{1}H/^{1}H 2D ROESY contour map of SRT:βCD IC at 1:1 molar ratio in D_2O and the expansion contour map for the aliphatic and aromatic region of SRT are depicted in Fig. 7a–c, respectively. Fig. 7a shows the contour map and cross peak correlations between βCD internal hydrogens (H3; H5) and aliphatic and aromatic SRT hydrogens. These cross peaks correlation of SRT aliphatic can be seen in the expansion contour map, in Fig. 7b. The cross peak correlation of the internal βCD hydrogens (H3; H5) occur with those SRT aliphatic hydrogens H2′ and H17, however, hydrogens H1′, H3′, and H4′ do not present dipolar cross peaks correlation with βCD hydrogens.

Another 2D ROESY expansion contour map of SRT aromatic hydrogens is presented in Fig. 7c. An intense cross peaks between H5′and H16 aromatic hydrogens of SRT was observed with H3 and H5 βCD internal hydrogens. Once H5′and H16 aromatic hydrogens are bonded in aromatic rings A and B, respectively, these cross peaks suggest that βCD interacts with two SRT molecular sites. This result suggests the existence of SRT:βCD ICs with 1:2 stoichiometry and/or existence of an multi-equilibrium system at 1:1 and 1:2 molar ratio, in accordance with FTIR-HATR and ITC experiments. However, even using a powerful NMR technique (2D ROESY), which demonstrated the binding sites between host and guest molecules a precisely information concerning the

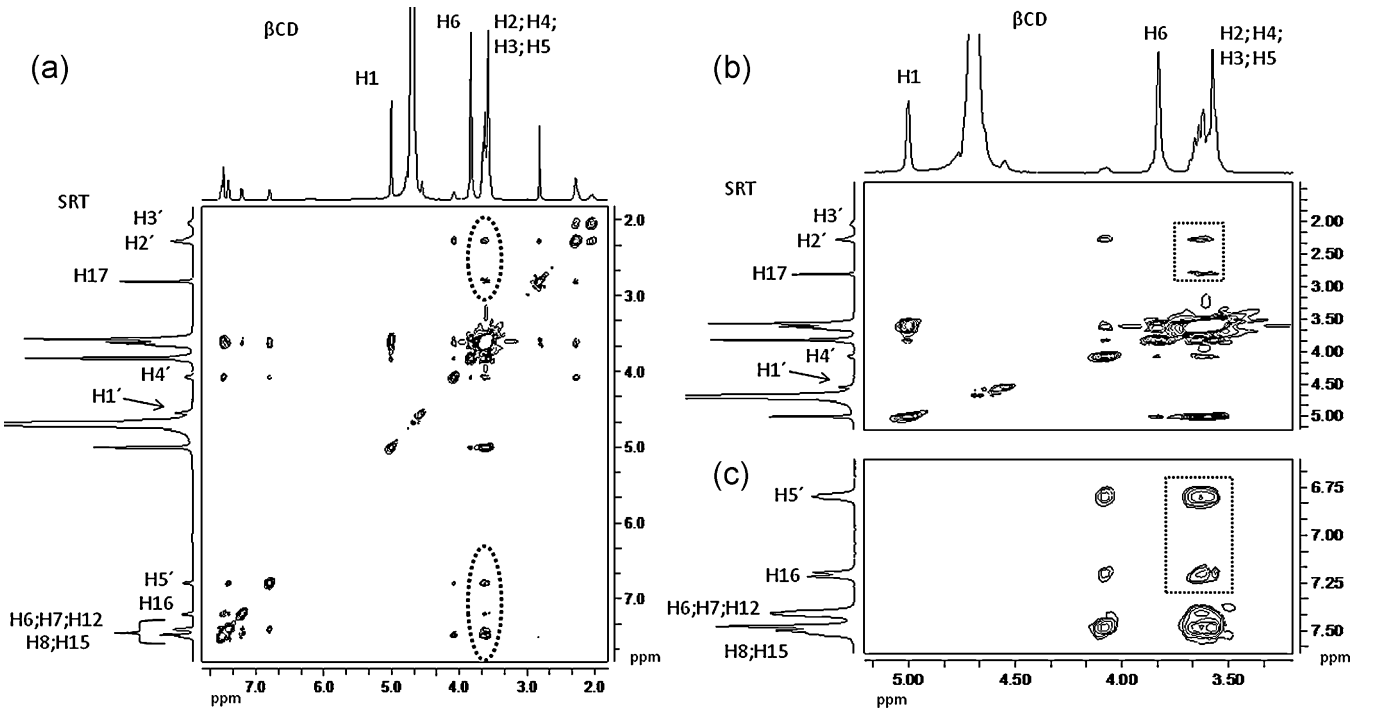

Fig. 7. (a) $^{1}H/^{1}H$ 2D-ROESY contour maps in D_2O (400 MHz) of IC at 1:1 molar ratio (b); expansion of the aliphatic region δ 3.20–5.20 and δ 6.60–7.60 and (c) expansion of the aromatic region δ 3.20–5.20 and δ 6.60–7.60.

supramolecular structure could not be achieved. To predict the most favorable supramolecular complex structure theoretical calculations were done to SRT:βCD ICs at different molar ratios and assuming a variety of spatial arrangements.

3.5. Theoretical calculations

A theoretical investigation at a molecular level is an additional and complementary tool to elucidate the structure of the ICs. Over the past few years, we have been working jointly using experimental and calculated data to define the geometry of these supramolecular arrangements (De Sousa et al., 2008b). The experimental results enable us to rationalize the stoichiometry relationship between the host and guest molecules, and also the most preferred inclusion modes and theoretical calculations allow us to evaluate the specific sites of interactions upon inclusion. In particular, these antidepressant molecules have as the key factor for their activity the distance between the center of the aromatic ring and the basic nitrogen atom that could be affected by the CDs environment (Chang et al., 1993; Dalpiaz et al., 1996).

Following the PM3 energetic data presented in Table 2, one can see that among all 1:1 SRT/βCD calculated structures, the IC IV (Fig. 2) is the most stable, and is quite close to second most stable complex VIII, with the relative energy difference between them being 2.3 kJ mol^{-1}. These two complexes are related to the inclusion of the aliphatic group, when the interaction is toward the larger and smaller rim of βCD, respectively. This energetic similarity is also noticed for the pairs of complexes: VII and III, when both phenyl and unsaturated rings (A and B, Fig. 1a) are enclosed by the βCD cavity. Complex VII, which relates that narrower rim inclusion, is 5.0 kJ mol^{-1} more stable than the wider one. When the analysis refers to all the complexes modeled, one can infer that 1:2 SRT/βCD X is the most stable complex. This stabilization is noticed due to the fitting of the SRT molecule inside both βCD cavities, also allowing closer interactions between the primary hydroxyls groups. Some C–H···O hydrogen bonds that frequently occur in carbohydrates and can influence the conformation of the host-guest selectivity are also present in this complex between the CDs unities, as well as, with the aliphatic methyl and the primary OHs. The energetic variation within the 1:2 complexes is more drastic than that observed in the 1:1 set. This may be due to the different kind of intermolecular interactions defined in the 1:2 complexes that include the CD–CD contacts. Complex II is the most unstable calculated structure ($\Delta\Delta E$ = 87.2 kJ mol^{-1}), and probably this is a result of a shallow inclusion of the dichlorophenyl ring regardless of the high potential for an inclusion trough the βCD larger rim. The superficial interaction is also the reason for the complex XIV to be the least stable among the 1:2 set. All PM3 optimized ICs are represented in the supporting material (see figure in Supplementary Data 4).

The structure of the three most stable complexes, X, IV and VIII, were reoptimized at the DFT level, using the reasonable 6-31G(d,p) basis set. For these DFT optimized complexes we also performed a vibrational analysis at the same theoretical level, which requires a large amount of computer time. The final geometries, which are true local minima, having no imaginary frequencies, are presented in Fig. 8. There are no drastic differences in the structures when comparing to the PM3 results, however, the thermodynamics has some variations without changing the relative stabilization order. These parameters are shown in Tables 2 and 3. For the DFT results, the distinction between the larger rim and smaller rim inclusion at 1:1 stoichiometry is more pronounced, with the wider inclusion (complex IV), being 35.6 kJ mol^{-1} more stable than the narrower one in complex VIII. Comparing complex IV with complex X, the 1:2 arrangement is still the most stable, however, the DFT energy difference is just 7.6 kJ mol^{-1}, which indicate a major equilibrium of these two species.

It is important to mention that water plays an important role in the complexes stabilization, and the implicit solvent model (PCM), in spite of its robustness, does not include the important water molecules that are inside the βCD cavity. Since, these results are calculated by the relative difference between products and reactants, we expect that error should be cancelled out. Keeping this in mind, complex X is still the most stable of the set, and the implicit

Table 2
Calculated thermodynamic data of the inclusion complex formation according to the equation: $n\beta CD + SRT \rightarrow n\beta CD\cdots SRT$ in gas phase at PM3 level and $T = 298.15$ K.

Inclusion complex	ΔE(kJ mol^{-1})	$\Delta\Delta E$(kJ mol^{-1})	ΔG(kJ mol^{-1})	ΔH(kJ mol^{-1})	$-T\Delta S$(kJ mol^{-1})
1:1 SRT:βCD					
I	−41.5	71.2	41.5	−34.4	75.9
II	−25.4	87.2	31.6	−19.8	51.4
III	−53.3	59.3	24.6	−46.7	71.3
IV	−68.7	43.9	30.2	−59.2	89.4
V	−50.1	62.5	45.6	−41.3	86.9
VI	−42.6	70.1	41.0	−34.2	75.2
VII	−58.3	54.4	30.8	−50.5	81.3
VIII	−66.4	46.3	28.5	−56.1	84.6
1:2 SRT:βCD					
IX	−89.7	22.9	154.8	−67.8	222.6
X	−112.6	0	83.3	−96.9	180.3
XI	−72.7	39.9	156.4	−57.9	214.2
XII	−86.5	26.2	133.9	−68.8	202.7
XIII	−69.1	43.6	95.1	−58.7	153.8
XIV	−65.7	46.9	85.6	−54.9	140.5
XV	−84.3	28.4	80.6	−72.6	153.3
XVI	−77.4	35.2	93.5	−63.3	156.8

Table 3
Calculated thermodynamic data of the inclusion complex formation according to the equation: $n\beta CD + SRT \rightarrow n\beta CD\cdots SRT$. Results for complexes X, IV and VIII at DFT/6-31G(d,p) level and $T = 298.15$ K.

ICs	ΔE(kJ mol^{-1})	$\Delta\Delta E$(kJ mol^{-1}	ΔG(kJ mol^{-1}	ΔH(kJ mol^{-1}	$-T\Delta S$(kJ mol^{-1}	ΔE_{sol}(kJ mol^{-1}
			1:1 SRT:βCD			
IV	−53.0	7.6	8.5	−38.7	47.3	–
VIII	−17.4	43.2	34.7	−11.0	45.8	–
			1:2 SRT/βCD			
X	−60.6	0	80.8	−41.0	121.8	–

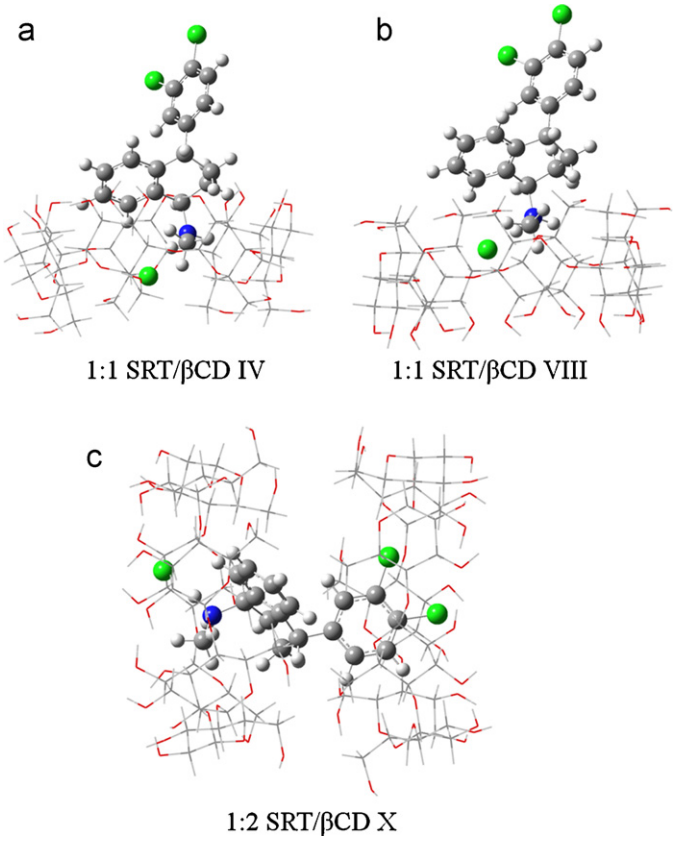

Fig. 8. Optimized PBE1PBE/6-31G(d,p) geometries for the most stable ICs at 1:1 SRT/βCD (a), IV (b) VIII and at 1:2 SRT/βCD (c) X.

solvation yields an additional stabilization of 102.1 kJ mol^{-1} to the electronic plus nuclear–nuclear repulsion energy value, if compared to the one in gas phase.

It is clear that the enthalpy variation shows an exothermic process, as well as, recognized by ITC results. The enthalpic contribution involves the formation or destruction of intermolecular interactions. Interestingly, the enthalpy variation on the IC formation is quite similar between some 1:1 and 1:2 compounds. In this case, as mentioned before, the lack of a more sophisticated solvent model is not a big problem due to the error cancellation. In spite of this, the calculated entropic contribution shows quite a different magnitude as well as sign, which is mostly due to the absence degree of freedom of the explicit water molecules in the model. In the experimental procedure, both SRT and βCD were highly hydrated, previous to the IC formation, and there were highly ordered water molecules around both molecules. Upon inclusion, the solvation shells are individually reorganized favoring the ΔG of the supramolecular complex. The most stable complexes predicted by the theoretical calculations are in structural agreement with the experimental data, suggesting an 1:1 and 1:2 equilibrium, especially for complex X that shows a complete inclusion of SRT by two βCDs simultaneously, enclosing both phenyl rings and also the aliphatic chain.

4. Conclusions

In this work the IC between SRT and βCD were obtained and the system was characterized by different methods. The results of these techniques suggest that this supramolecular system presents a 1:1 and 1:2 SRT:βCD stoichiometries in equilibrium simultaneously in aqueous solutions. The IC obtained was more soluble than free SRT in different biomimetic fluids and this solubility enhances when βCD molar ratio increases. SRT:βCD interaction was confirmed by the βCD νC–O–C stretching modes reduction, allowing to estimate

the IC stoichiometry in solution. ITC experiments demonstrated that SRT and βCD inclusion process is exothermic and spontaneous, accompanied by high affinity binding constant. IC formation was driven by entropy and the hydrophobic interaction between the SRT and βCD was predominant. The stoichiometry coefficient determined by ITC experiments is supported by FTIR-HATR titration and Job's plot. ^{1}H NMR experiments evidenced the SRT and βCD interactions based on the hydrogens chemical shift. Moreover, 2D ROESY contour maps showed mainly cross peaks correlations between SRT aromatic hydrogens and the internal βCD hydrogens. Theoretical calculations were useful to elucidate the most energetically stable structures among the multiple inclusion possibilities. From these results, one can infer that the 1:2 inclusion is the most stable, but do not discard equilibrium with 1:1 complexes as well as observed in experimental data.

Acknowledgments

We would like acknowledge financial support by Brazilian agencies CAPES, CNPq, FAPEMIG and INCT-NanoBiofar. The authors want to acknowledge the support of the Chemistry Department from Federal University of Minas Gerais, Brazil.

Appendix A. Supplementary data

Supplementary data associated with this article can be found, in the online version, at doi:10.1016/j.ijpharm.2011.09.026.

References

(CSD):http://www.ccdc.cam.ac.uk/, C.S.D.
Baka, E., Comer, J.E.A., Takács-Novák, K., 2008. Study of equilibrium solubility measurement by saturation shake-flask method using hydrochlorothiazide as model compound. J. Pharmaceut. Biomed. Anal. 46, 335–341.
Bouchemal, K., 2008. New challenges for pharmaceutical formulations and drug delivery systems characterization using isothermal titration calorimetry. Drug Discov. Today 13, 960–972.
Brewster, M.E., Loftsson, T., 2007. Cyclodextrins as pharmaccutical solubilizers. Adv. Drug Deliv. Rev. 59, 645–666.
Burke, K., Perdew, J.P., Wang, Y., 1988. Eletronic Density Functional Theory: Recent Progress and New Directions. Springer.
Cances, E., Mennucci, B., Tomasi, J., 1997. A new integral equation formalism for the polarizable continuum model: theoretical background and applications to isotropic and anisotropic dielectrics. J. Chem. Phys. 107, 3032–3041.
Cannavà, C., Crupi, V., Ficarra, P., Guardo, M., Majolino, D., Stancanelli, R., Venuti, V., 2008. Physicochemical characterization of coumestrol/[beta]-cyclodextrins inclusion complexes by UV–vis and FTIR-ATR spectroscopies. Vib. Spectrosc. 48, 172–178.
Caruso, F., Besmer, A., Rossi, M., 1999. The absolute configuration of sertraline (Zoloft) hydrochloride. Acta Crystallogr. C: Cryst. Struct. Commun. 55, 1712–1714.
Chang, A.S.S., Chang, S.M., Starnes, D.M., 1993. Structure–activity-relationships of serotonin transport—relevance to nontricyclic antidepressant interactions. Eur. J. Pharmacol.: Mol. Pharmacol. Sect. 247, 239–248.
Dalpiaz, A., Ferretti, V., Gilli, P., Bertolasi, V., 1996. Stereochemistry of serotonin receptor ligands from crystallographic data. Crystal structures of NAN-190. HBr, 1-phenylbiguanide, MDL 72222 and mianserin. HCl and selectivity criteria towards 5-HT1, 5-HT2 and 5-HT3 receptor subtypes. Acta Crystallogr. B: Struct. Commun. 52, 509–518.
Davis, M.E., Brewster, M.E., 2004. Cyclodextrin-based pharmaceutics: past, present and future. Nat. Rev. Drug Discov. 3, 1023–1035.
Araujo, M.V., Vieira, E.K., Lazaro, S., Conegero, L.D.S., Ferreira, O.P., Almeida, L.E., Barreto, L.S., Costa, N.B., Gimenez, I.F., 2007. Inclusion complexes of pyrimethamine in 2-hydroxypropyl-beta-cyclodextrin: characterization, phase solubility and molecular modelling. Bioorgan. Med. Chem. 15, 5752–5759.
De Sousa, F.B., Denadai, Â.M.L., Lula, I.S., Ianzer, D., Malaspina, E.R., Camargo, A.C.M., dos Santos, R.A.S., Sinisterra, R.D., 2010a. Structural and physical–chemical evaluation of Bradykinin potentiating peptide and its high soluble supramolecular complex. J. Inclusion Phenom. Macrocycl. Chem. 67, 407–422.
De Sousa, F.B., Denadai, Â.M.L., Lula, I.S., Lopes, J.F., Dos Santos, H.F., De Almeida, W.B., Sinisterra, R.D., 2008a. Supramolecular complex of fluoxetine with beta-cyclodextrin: an experimental and theoretical study. Int. J. Pharm. 353, 160–169.
De Sousa, F.B., Denadai, Â.M.L., Lula, I.S., Nascimento Jr., C.S., Fernandes, N.S.G., Lima, A.C., De Almeida, W.B., Sinisterra, R.D., 2008b. Supramolecular self-assembly of cyclodextrin and higher water soluble guest: thermodynamics and topological studies. J. Am. Chem. Soc. 130, 8426–8436.
De Sousa, F.B., Guerreiro, J.D.T., Ma, M.L., Anderson, D.G., Drum, C.L., Sinisterra, R.D., Langer, R., 2010b. Photo-response behavior of electrospun nanofibers based on spiropyran–cyclodextrin modified polymer. J. Mater. Chem. 20, 9910–9917.
De Sousa, F.B., Oliveira, M.F., Lula, I.S., Sansiviero, M.T.C., Cortes, M.E., Sinisterra, R.D., 2008c. Study of inclusion compound in solution involving tetracycline and beta-cyclodextrin by FTIR-ATR. Vib. Spectrosc. 46, 57–62.
Denadai, Â.M.L., Teixeira, K.I., Santoro, M.M., Pimenta, A.M.C., Cortes, M.E., Sinisterra, R.D., 2007. Supramolecular self-assembly of beta-cyclodextrin: an effective carrier of the antimicrobial agent chlorhexidine. Carbohydr. Res. 342, 2286–2296.
Ditchfield, R., Hehre, W.J., Pople, J.A., 1971. Self-consistent molecular-orbital methods. IX. An extended Gaussian-type basis for molecular-orbital studies of organic molecules. J. Chem. Phys. 54, 724–728.
Fernandes, C.M., Carvalho, R.A., da Costa, S.P., Veiga, F.J.B., 2003. Multimodal molecular encapsulation of nicardipine hydrochloride by beta-cyclodextrin, hydroxypropyl-beta-cyclodextrin and triacetyl-beta-cyclodextrin in solution. Structural studies by H-1 NMR and ROESY experiments. Eur. J. Pharm. Sci. 18, 285–296.
Frisch, M.J., Trucks, G.W., Schlegel, H.B., Scuseria, G.E., Robb, M.A., Cheeseman, J.R., M.J., J.A., Vreven, T., Kudin, K.N., Burant, J.C., Millam, J.M., Iyengar, S.S., Tomasi, J., Barone, V., Mennucci, B., Cossi, M., Scalmani, G., Rega, N., Petersson, G.A., Nakatsuji, H., Hada, M., Ehara, M., Toyota, K., Fukuda, R., Hasegawa, J., Ishida, M., Nakajima, T., Honda, Y., Kitao, O., Nakai, H., Klene, M., Li, X., Knox, J.E., Hratchian, H.P., Cross, J.B., B., V., Adamo, C., Jaramillo, J., Gomperts, R., Stratmann, R.E., Yazyev, O., Austin, A.J., Cammi, R., Pomelli, C., Ochterski, J.W., Ayala, P.Y., M., K., Voth, G.A., Salvador, P., Dannenberg, J.J., Zakrzewski, V.G., D., S., Daniels, A.D., Strain, M.C., Farkas, O., Malick, D.K., Rabuck, A.D., Raghavachari, K., Foresman, J.B., Ortiz, J.V., Cui, Q., Baboul, A.G., C., S., Cioslowski, J., Stefanov, B.B., Liu, G., Liashenko, A., Piskorz, P., Komaromi, I., Martin, R.L., Fox, D.J., Keith, T., Al-Laham, M.A., P., C.Y., Nanayakkara, A., Challacombe, M., Gill, P.M.W., Johnson, B., C., W., Wong, M.W., Gonzalez, C., Pople, J.A, 2004. Gaussian 2003, Revision C.02., Wallingford, CT.
Gottlieb, H.E., Kotlyar, V., Nudelman, A., 1997. NMR chemical shifts of common laboratory solvents as trace impurities. J. Org. Chem. 62, 7512–7515.
Harada, A., Kobayashi, R., Takashima, Y., Hashidzume, A., Yamaguchi, H., 2011. Macroscopic self-assembly through molecular recognition. Nat. Chem. 3, 34–37.
Hehre, W.J., Ditchfield, R., Pople, J.A., 1972. Self-consistent molecular orbital methods. XII. Further extensions of Gaussian—type basis sets for use in molecular orbital studies of organic molecules. J. Chem. Phys. 56, 2257–2261.
Hörter, D., Dressman, J.B., 2001. Influence of physicochemical properties on dissolution of drugs in the gastrointestinal tract. Adv. Drug Deliv. Rev. 46, 75–87.
Johnson, B.M., Chang, P.-T.L., Harry, G.B., 1996. Sertraline Hydrochloride, Analytical Profiles of Drug Substances and Excipients. Academic Press, pp. 443–486.
Jullian, C., Orosteguis, T., Pérez-Cruz, F., Sánchez, P., Mendizabal, F., Olea-Azar, C., 2008. Complexation of morin with three kinds of cyclodextrin: a thermodynamic and reactivity study. Spectrochim. Acta A: Mol. Biomol. Spectr. 71, 269–275.
Lindner, K., Saenger, W., 1982. Crystal and molecular-structure of cycloheptaamylose dodecahydrate. Carbohydr. Res. 99, 103–115.
Loftsson, T., Duchene, D., 2007. Cyclodextrins and their pharmaceutical applications. Int. J. Pharm. 329, 1–11.
Marques, F.D., Ferreira, A.J., Sinisterra, R.D.M., Jacoby, B.A., Sousa, F.B.D., Caliari, M.V., Silva, G.A.B., Melo, M.B., Nadu, A.P., Souza, L.E., Irigoyen, M.C.C., Almeida, A.P., Santos, R.A.S., 2011. An oral formulation of angiotensin-(1–7) produces cardioprotective effects in infarcted and isoproterenol-treated rats. Hypertension 57, 477–483.
Messner, M., Kurkov, S.V., Jansook, P., Loftsson, T., 2010. Self-assembled cyclodextrin aggregates and nanoparticles. Int. J. Pharm. 387, 199–208.
Nouws, H.P.A., Delerue-Matos, C., Barros, A.A., Rodrigues, J.A., 2005. Electroanalytical study of the antidepressant sertraline. J. Pharm. Biomed. Anal. 39, 290–293.
Panchagnula, R., Thomas, N.S., 2000. Biopharmaceutics and pharmacokinetics in drug research. Int. J. Pharm. 201, 131–150.
Perdew, J.P., Burke, K., Ernzerhof, M., 1996. Generalized gradient approximation made simple. Phys. Rev. Lett. 77, 3865.
Perdew, J.P., Burke, K., Ernzerhof, M., 1997. Generalized gradient approximation made simple. Phys. Rev. Lett. 78, 1396 (vol 77, pg 3865, 1996).
Rekharsky, M.V., Inoue, Y., 1998. Complexation thermodynamics of cyclodextrins. Chem. Rev. 98, 1875–1917.
Schneider, H.J., Hacket, F., Rudiger, V., Ikeda, H., 1998. NMR studies of cyclodextrins and cyclodextrin complexes. Chem. Rev. 98, 1755–1785.
Stewart, J.J.P., 1989. Optimization of parameters for semiempirical methods. 2. Applications. J. Comput. Chem. 10, 221–264.
Sun, D.Z., Li, L., Qiu, X.M., Liu, F., Yin, B.L., 2006a. Isothermal titration calorimetry and H-1 NMR studies on host–guest interaction of paeonol and two of its isomers with beta-cyclodextrin. Int. J. Pharm. 316, 7–13.
Sun, D.Z., Qiu, X.M., Li, L., Wei, X.L., Yin, B.L., 2006b. A study of alpha-cyclodextrin with a group of cationic gemini surfactants utilizing isothermal titration calorimetry and NMR. J. Chem. Thermodyn. 38, 773–777.
Sutton, S.C., Evans, L.A., Fortner, J.H., McCarthy, J.M., Sweeney, K., 2006. Dog colonoscopy model for predicting human colon absorption. Pharm. Res. 23, 1554–1563.
Szejtli, J., 1998. Introduction and general overview of cyclodextrin chemistry. Chem. Rev. 98, 1743–1753.
Takács-Novák, K., Tihanyi, K., Noszál, B., Deák, K., 2006. Physico-chemical profiling of antidepressive sertraline: solubility, ionization, lipophilicity. Med. Chem. 2, 385–389.
Uekama, K., Hirayama, F., Irie, T., 1998. Cyclodextrin drug carrier systems. Chem. Rev. 98, 2045–2076.